Charge-induced formation of linear Au clusters on thin MgO films: Scanning tunneling microscopy and density-functional theory study

Violeta Simic-Milosevic,[1] Markus Heyde,[1] Xiao Lin,[1] Thomas König,[1] Hans-Peter Rust,[1] Martin Sterrer,[1] Thomas Risse,[1] Niklas Nilius,[1,*] Hans-Joachim Freund,[1] Livia Giordano,[2] and Gianfranco Pacchioni[2,†]

[1]*Department of Chemical Physics, Fritz-Haber-Institut der Max-Planck-Gesellschaft, Faradayweg 4-6, D-14195 Berlin, Germany*
[2]*Dipartimento di Scienza dei Materiali, Università di Milano–Bicocca, I-20125 Milano, Italy*

Gold deposition onto ultrathin MgO films on Ag(001) results in the formation of linear Au clusters, as revealed from a combined scanning tunneling microscopy and density-functional theory study. The equilibrium structure of small Au clusters containing three to seven atoms is therefore different on thin film and bulk MgO(001) but also deviates from the shape of the respective gas-phase clusters. The peculiar one-dimensional growth regime of gold is stimulated by an electron transfer from the MgO/Ag interface to the deposited Au clusters, resulting in singly and doubly charged cluster anions. Only for larger atom numbers, the formation of compact two-dimensional clusters prevails on the MgO thin films.

I. INTRODUCTION

The electronic and geometric structure of gold clusters deposited on oxide surfaces is attracting an increasing interest in both catalysis and surface science communities.[1] The surprising discovery that once in the form of nanoparticles even this inert metal becomes an active catalyst[2,3] has stimulated many attempts to elucidate the reasons for the enhanced reactivity. So far, the chemical properties of nanostructured gold have been related to the nature and pretreatment of the oxide support,[4] as well as to the size and shape of the deposits.[5] Also the charge state of Au species is assumed to play a decisive role. While some studies suggest $Au^{\delta+}$ (cationic gold) to be the active phase,[6–8] in other cases, negatively charged clusters, both in the gas phase[9] and on oxide supports,[10,11] were found to be more active than their positively charged or neutral counterparts. In a widely accepted picture, the excess charges facilitate the breaking of bonds in molecules adsorbed on the Au deposits and hence lower the activation barrier for surface reactions.

Anionic gold species can be produced in various ways. On bulklike oxides, e.g., MgO and TiO_2, charging occurs due to electron transfer from electron-rich surface defects, e.g., oxygen vacancies, as demonstrated by density-functional theory (DFT) calculations and CO vibrational spectroscopy.[12–14] An alternative charging mechanism prevails on ultrathin oxide films (MgO and FeO) grown on metal supports.[15,16] Here, electrons are transferred into initially unoccupied affinity levels of the adsorbate via tunneling from the metal support. The electron flow is facilitated by a work function reduction that often accompanies the growth of thin oxide films on metal surfaces, as shown for MgO films on Ag(001) and Mo(001).[17–19] The charging of electronegative species on thin oxide films therefore follows the oxidation model for metals developed by Cabrera and Mott.[20]

Negative charging of individual Au adatoms and clusters has been demonstrated, both experimentally and theoretically, for a few oxide films. Single Au atoms deposited on MgO thin films on Ag(001) self-assemble into a hexagonal array of adatoms, indicating the presence of Coulomb repulsion between the negatively charged species.[21] With increasing exposure, two-dimensional (2D) Au islands form on the oxide film,[22] although Volmer-Weber growth is typically observed for Au on bulk MgO. The deviating growth regime provides additional evidence for the accumulation of extra electrons in the Au aggregates, enabling enhanced polarization interactions and thus stronger binding to the oxide surface.[23,24] Recent non-spin-polarized DFT studies have shown that also Au clusters containing up to six atoms become negatively charged on MgO/Mo(001) films.[24,25] On alumina thin films grown on NiAl(110), the charge transfer into the Au could even be quantified, thanks to the unique shape of the adclusters.[26] The Au atoms self-assemble into one-dimensional (1D) chains on this surface and develop distinct quantum well states due to the overlap of the Au 6s orbitals in neighboring chain atoms. By comparing the electron filling of those states with the number of 6s electrons in the initial gas-phase clusters, the amount of charge transfer was determined to range between one and three electrons depending on the chain length.[27] Although not proven experimentally, the formation of negatively charged Au species is expected to increase the reactivity of thin-film systems, opening a promising way to tune the catalytic performance of such composite materials.[28,29]

In this paper, we report on a combined scanning tunneling microscopy (STM) and DFT study of the properties of Au clusters formed on ultrathin MgO films on Ag(001). The clusters spontaneously adopt 1D shapes upon Au deposition but also arrange in a linear way during manipulation experiments performed with the STM tip. The distinct structural properties are confirmed by DFT calculations and traced back to a negative charging of the adchains. Au on MgO/Ag(001) behaves therefore similar to the alumina on NiAl(110) case, providing another example for the "unusual" nature of gold on thin oxide films.

II. EXPERIMENTAL AND COMPUTATIONAL DETAILS

The experiments were performed in a custom-built Eigler style ultrahigh-vacuum STM operating at 5 K.[30] The Ag(001)
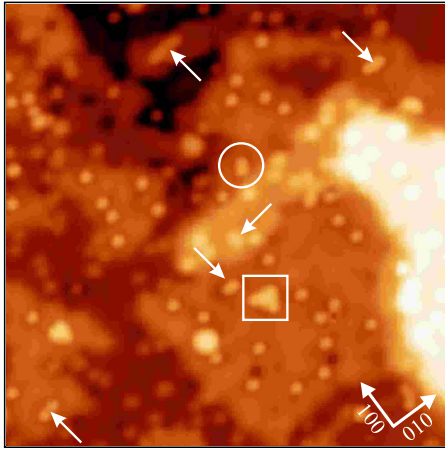
FIG. 1. (Color online) STM topographic image of Au adatoms and clusters on a 2-ML-thick MgO film on Ag(001) (−0.4 V, 19 ×19 nm^2). The arrows mark [100]- and [010]-oriented Au chains, while the circle depicts a chain in the [110] direction. The square frames a triangular 2D cluster.
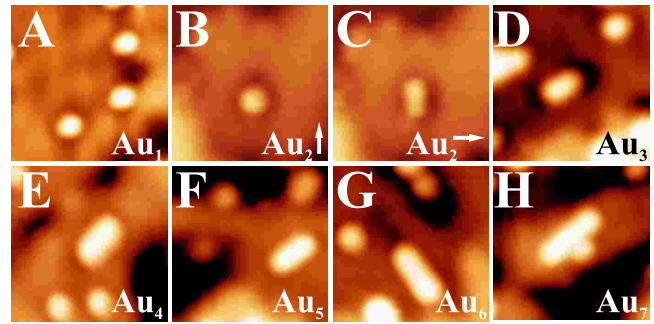

FIG. 2. (Color online) STM topographic images of (A) Au monomers, [(B) and (C)] upright and flat Au dimers, and [(D)–(H)] Au chains containing three to seven atoms on MgO/Ag(001) (−0.4 V, 5×5 nm^2).

sample was cleaned by repeated cycles of Ar$^+$ sputtering (500 eV and 10 μA) and annealing to 700 K. MgO films of 2–3 ML thickness were prepared by reactive Mg deposition at 570 K in an oxygen ambiance of 1×10^{-6} mbar. Single Au atoms were deposited from a high-purity wire (99.95%) wrapped with a tungsten filament onto the sample surface held at 100 K. The deposition temperature was therefore higher than in previous experiments to enforce the development of Au equilibrium structures on the oxide surface.[13,21,31] The coverage was adjusted between 0.01 and 0.02 ML. Whereas at low coverage, Au monomers are the predominant surface species, a large collection of differently shaped aggregates appear at higher Au exposure.

The DFT calculations were performed in the generalized gradient approximation (PW-91 exchange-correlation functional)[32] as implemented in the VASP code.[33,34] A plane-wave basis set (400 eV energy cutoff) and the projected augmented wave (PAW) method[35] were used for the core electrons. The substrate was modeled by four Ag(001) planes, adding two MgO layers to one side of the slab. The residual dipoles perpendicular to the surface were eliminated with a specific dipole correction scheme. To account for the differently sized Au clusters, (3×3), (4×4), and (5×5) supercells were constructed. Only for Au$_5$ and Au$_6$ chains, the use of a (4×7) cell became necessary. The atoms in the supercells were relaxed until the atomic forces fell below 0.01 eV/Å. The electronic properties were determined by Brillouin-zone integrations on a (4×4×1) Monkhorst-Pack grid[36] for the (3×3) cell, while an equally spaced k-point sampling was applied to larger unit cells. Except for the largest cell, calculations were carried out in a spin-polarized scheme in order to account for the possible presence of unpaired electrons in the valence shell of the Au clusters.

A. Experimental results

Figure 1 shows a typical STM topographic image of a 2-ML-thick MgO film on Ag(001) after deposition of 0.02

ML of Au. The majority species are round protrusion of 0.8 Å height, which are assigned to single Au adatoms. Also differently shaped Au aggregates are found in the images, for instance small triangular-shaped clusters (see square in Fig. 1). The focus of this paper is, however, chainlike Au aggregates, which are frequently observed on the MgO surface (arrows in Fig. 1). Most of the chains align with the MgO [100] and [010] directions, which is the crystallographic orientation where Mg and O atoms alternate on the surface. However, also [110] oriented Au chains are found on the thin MgO film (circle in Fig. 1).

Seven different chains could be discriminated in the images on the basis of their length (Fig. 2). The largest one is approximately 22 Å long when measuring the distance between the two terminal points on which the topographic chain height reaches 50% of its maximum value. For each shorter chain, the length reduces by 2.5–3.0 Å, getting down to the Au monomer that is characterized by a spherical shape and 6 Å apparent diameter. According to this length estimate, the longest chain on the MgO surface corresponds to a Au heptamer (Au$_7$), while the most frequent ones are trimer and tetramer chains. In the bias window available for surface imaging (−1.0 to +1.0 V), single atoms and Au chains have similar apparent heights of 0.8 Å. The only exception is a small spherical Au species that is approximately 40% higher than the monomer [Fig. 2(B)].[31]

The electronic properties of linear Au clusters were investigated with differential conductance (dI/dV) spectroscopy. Independent of the chain length, the spectra did not reveal peaks in the conductance and were similar to the ones taken on the bare MgO film (Fig. 3). Apparently, no initial or final states are available for tunneling into or out of the adstructures, as also suggested by their uniform apparent height in STM imaging. Only in dI/dV maps taken at negative bias, a small increase in the signal becomes visible at both sides of longer chains [Figs. 3(A) and 3(B)]. It should be mentioned at this point that conductance measurements were hampered by the small bias window available for spectroscopy (±1.0 V). Applying bias values outside this range usually caused the alteration of the Au aggregates, as manifested by their desorption, motion, or dissociation.

The high susceptibility of oxide-supported Au atoms to the electron injection was, however, exploited to manipulate
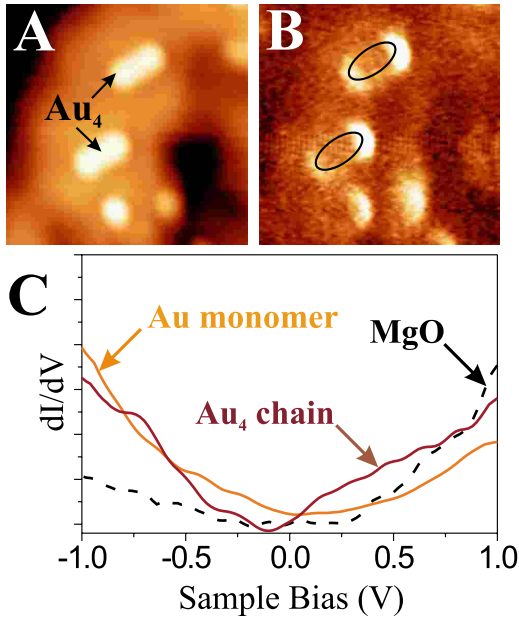
FIG. 3. (Color online) (A) Topographic and (B) differential conductance images of two Au_4 chains on MgO/Ag(001) (-0.4 V, 6.5×6.5 nm^2). (C) dI/dV spectra of a monomer and an Au_4 chain (set point bias of $+0.8$ V). Apart from the end states in (B), no dI/dV features are visible in spectroscopy within the accessible bias window.

their binding configuration and spatial arrangement on the surface. For this purpose, the tip was positioned above a selected Au species (a single atom or an aggregate) and the voltage was increased above the manipulation threshold (usually to 2.0 V) with enabled feedback loop. A sudden decrease in the tip height manifested the success of the manipulation experiment and a change in the adsorbate structure. In the majority of cases, the manipulation procedure led to the displacement of Au atoms in a large area below the tip position. The required atom mobility was hereby generated by the tip-induced electric field or alternatively by the temporal occupation of mixed Au-MgO states with antibonding character. In few examples, Au monomers aggregated upon electron injection (Fig. 4). Surprisingly, also these artificial clusters adopted 1D shapes, manifesting the thermodynamic preference for the Au chain formation on thin MgO films. The strong trend for a linear arrangement of Au atoms on MgO/Ag(001) and the properties of the resulting adchains
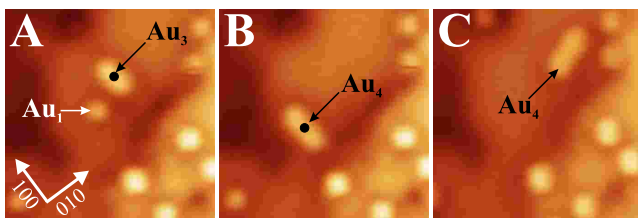

FIG. 4. (Color online) (A) STM image showing a trimer and monomers on the MgO film. (B) A $+2$ V bias pulse was applied to the trimer at the position marked by the black dot, creating a tetramer chain. (C) The same manipulation procedure was repeated for the tetramer, inducing the diffusion of the adchain.
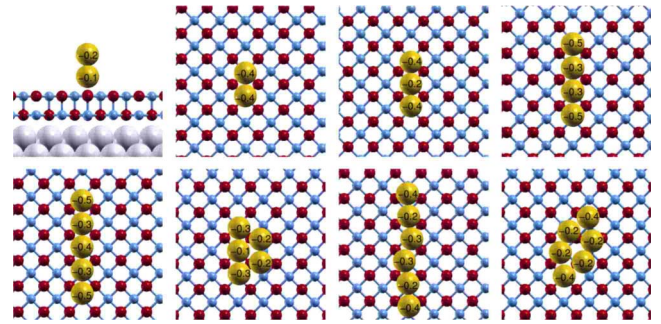

FIG. 5. (Color online) Most stable Au_n isomers ($n=2-6$) on 2 ML MgO/Ag(001). Red spheres: O atoms; blue spheres: Mg atoms; yellow spheres: Au atoms. Bader charges are displayed on the corresponding Au atoms (in $|e|$).

shall be discussed in the light of DFT calculations in the following.

B. Theoretical results

As discussed in earlier publications,[15,21,24] Au atoms are able to form strong bonds to a 2-ML-thick MgO film on Ag(001). The large increase in binding energy with respect to bulk MgO (1.5 versus 0.9 eV) originates from a negative charging of the adatom via electron transfer from the Ag support. The Au$^-$ species is able to lock into the Madelung field of the oxide film and induces a polaronic distortion of the MgO that enhances the polarization interaction with the adatom. The preferred Au binding sites are identified as the Mg^{2+} top site and the hollow site in the oxide surface, in contrast to bulk MgO where binding to the oxygen anions is clearly favored. The energetic preference of cationic over anionic sites is, however, small (0.25 eV) for the thin MgO film, leading to a flat potential-energy surface for adsorption.[15]

The smallest Au aggregate, the dimer, forms in two different configurations on the MgO/Ag(001) surface (Fig. 5).[31] In its most stable configuration, the Au_2 has an upright geometry with the lower atom attached to a surface oxygen ion ($r_{Au-Au}=252$ pm, $r_{Au-O}=217$ pm). The upright dimer is neutral and has a closed-shell electronic structure, in analogy to Au dimers on bulk MgO(001).[37] Furthermore, different flat-lying Au_2 species are stable on the thin film, which are either bound to two Mg^{2+} ions or to two hollow sites and align with the MgO[100] or [110] direction. In all cases, the flat Au_2 is slightly higher in energy (0.34 eV) than its upright counterpart and carries an additional electron ($-0.8e$), as deduced from a Bader charge analysis. A closer look to the charge-density difference reveals that the electron is transferred from the MgO/Ag interface region. The negative charging of the flat dimer is compatible with two additional observations, namely, the enlarged Au-Au distance of 264 pm (similar to a gas-phase Au_2^-) and the strong polaronic distortion of the MgO lattice around the anionic species. Since flat-lying Au_2^- cannot be stabilized on bulk MgO, the emergence of this species is directly related to the presence of the metal support below the oxide film and the associated charge transfer.
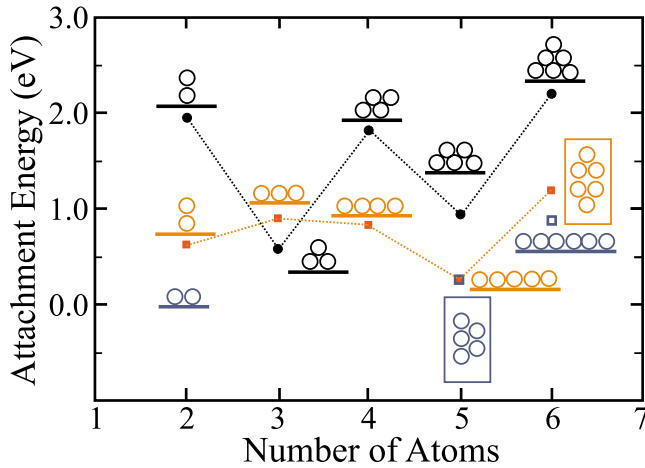
FIG. 6. (Color online) Calculated atom attachment energies to form the Au clusters shown in the insets, either for bulk MgO(001) (black circles) or for 2 ML MgO on Ag(001) (orange squares). The open squares depict the second most stable isomers on the thin film. While pronounced odd-even oscillations in the attachment energy are visible on bulk MgO, such behavior is suppressed on the thin film. This relates to the removal of most open-shell configurations by electron transfer trough the MgO film (e.g., for Au_3) and to the screening of unpaired electrons by the support for the remaining magnetic clusters (e.g., Au_5). Attachment energies on the thin film are also lower than on bulk MgO, as each aggregation step implies the bond formation between two charged species.

Despite this strong stabilization effect of the MgO/Ag(001) support, the neutral and upright Au_2 is the lowest-energy isomer and not the flat-lying species. This unexpected result is rationalized by the fact that the extra electron in the flat Au_2^- occupies an antibonding 6s-6s hybrid state and therefore weakens the interatomic interaction. The lower Au-Au binding energy is not compensated by the stronger adhesion to the surface and the flat-lying configuration remains energetically less favorable. Interestingly, the flat and upright dimers are nearly isoenergetic on MgO films on Mo(001), reflecting the even stronger impact of the Mo support on the Au-MgO interaction.[25] For both substrates, the thermodynamic stability of the flat-lying Au_2^- species decreases with increasing film thickness, demonstrating the diminishing influence of the metal support on the adhesion energy.

To characterize the nucleation behavior of dimers and larger Au aggregates on the MgO thin film, the attachment energy E_b of a single adatom to an existing Au_{n-1} cluster is calculated via

$$E_b(Au_n) = -E(Au_n/MgO) - E(MgO) + E(Au_{n-1}/MgO)$$
$$+ E(Au_1/MgO).$$

The formation energy for Au dimers on the 2 ML MgO/Ag(001) film is determined with 0.63 and 0.29 eV for the vertical and flat configurations, respectively (2.1 eV on bulk MgO) (Fig. 6). The low values reflect the rather small adhesion of neutral and singly charged dimers with respect to two negatively charged and hence strongly bound adatoms. During the aggregation process, also the Coulomb repulsion be-

tween the two Au^- species needs to be overcome and one electron has to be transferred back into the substrate, introducing an additional barrier for dimer formation. However, as the attachment energy is still positive, Au dimers are expected to form spontaneously on the MgO thin film.

In agreement with the DFT calculations, Au dimers in both the flat-lying and the upright configurations are unambiguously identified in STM images of the surface [Figs. 2(B) and 2(C)]. Whereas the flat-lying species shows up as ellipsoidal feature with 9 Å apparent length and 0.8 Å height, the vertical one is a round protrusions of 1.1 Å height.[31] In accordance to the theoretical predictions, the ellipsoidal structures assigned to flat dimers are less frequently observed on thin MgO films than the upright species, reflecting their lower thermodynamic stability and formation energy.

Adding a third Au atom to a vertical Au_2 dimer on 2 ML MgO/Ag(001) leads to the formation of a neutral upright Au triangle that is similar to the lowest-energy isomer on bulk MgO(001). However, a flat-lying Au_3 chain is by far more stable on the thin film than the upright triangle, in contrast to the dimer case (Fig. 5). In the lowest-energy configuration, the three atoms occupy neighboring MgO hollow sites in [100] direction. Two other geometries, where the trimer axis points along the [110] direction or the Au atoms sit atop Mg^{2+} sites, are almost isoenergetic (energy difference below 0.1 eV). The Au_3 chain carries one extra electron similar to the flat Au dimer, as proven by the Bader analysis, the polaronic distortion of the oxide lattice, and the absence of unpaired electrons in the trimer ground state. The clear preference for the formation of charged flat-lying Au_3 species is compatible with the high electron affinity of the trimer with respect to the dimer (3.7 versus 2.0 eV).[38] The stability of the Au_3^- chain on the thin-film support is also reflected by the high formation energy of 0.94 eV, which exceeds the one for triangular-shaped clusters on bulk MgO(001) by 60% (E_b =0.58 eV) (Fig. 6). Attempts to locate other triangular isomers that lie flat on the surface failed, as all structures spontaneously relaxed into the 1D configuration.

A linear cluster oriented along MgO[100] or [110] also represents the most stable configuration for the Au tetramer on the thin magnesia film (Fig. 5). The 1D structure is preferred by 0.8 eV over the standing rhombus, which is the lowest-energy isomer on bulk MgO(001). Also other possible configurations, such as a Y-shaped structure, were tested and found to be less stable by about 0.7 eV with respect to the chain. In contrast, the Y-shaped configuration has been proposed as the most stable isomer on Mo-supported MgO films, most likely due to the different nature of the MgO/Mo(001) interface.[24,25] It should be noted yet that the linear chain was not considered in that study. Similar to the dimer and trimer cases, the linear arrangement of atoms in Au_4 clusters is driven by a charge transfer from the metal support. However, even spin-polarized calculations of the tetramer chain yield a diamagnetic ground state, although the gas-phase cluster is a closed-shell system and the extra electron should therefore induce a magnetic moment. A plausible explanation for the nonmagnetic ground state is the transfer of two electrons from the Ag(001) support into the gold cluster, which is indeed confirmed by the Bader analysis (Fig. 5).

The presence of two extra electrons also explains the one-dimensional shape of the cluster, as only in this configuration the additional charge is optimally delocalized and the internal electrostatic repulsion is minimized. The tendency to separate the extra electrons is also reflected by the fact that the two terminal chain atoms carry higher fractional charges than the central ones (Fig. 5). As the charge distribution in a compact rhombus is less efficient, the total energy of 2D isomers is higher despite the larger number of internal Au-Au bonds. The Au_4 on MgO thin films is not the only example for a doubly charged tetramer chain as a similar species has recently been found on alumina thin films.[27]

Although formation of linear Au clusters on MgO/Ag(001) is favored for small atom numbers, the 1D growth has to pass into a 2D regime with increasing coverage, according to recent STM results.[22] Also DFT calculations revealed that gold clusters of 8–20 atoms deposited on ultrathin MgO films assume flat 2D structures, instead of the linear shapes obtained here.[23] It is thus instructive to analyze the size range, in which the transition between 1D and 2D growths occurs. For this purpose, the energy of Au_5 and Au_6 clusters on MgO/Ag(001) and bulk MgO(001) supports is determined for several linear and flat-lying 2D configurations (Fig. 5). On bulk MgO, none of these structures is adopted and Au clusters assume a flat shape with the plane normal to the surface.[39,40] On the thin film, on the other hand, 1D and flat-lying 2D isomers are found to be isoenergetic for the Au_5 species (Fig. 5). While the 2D aggregate is singly charged, the linear configuration accommodates two extra electrons that are mainly localized at the two terminal atoms (Fig. 5). The formation energy of a Au_5 chain is with 0.2 eV rather small, which relates to the energy cost to form a magnetic pentamer with a half-filled electronic state located at the Fermi level. Still, the linear Au_5 chain forms spontaneously on the surface but might represent a critical size where 1D cluster growth on MgO/Ag(001) breaks down.

This assumption is confirmed by the DFT results for different Au_6 isomers being the largest cluster considered in this work. The Au hexamer adsorbs preferentially in a flat 2D geometry (Fig. 5), which is 0.3 eV lower in energy than the 1D chain. Both conformers accommodate two extra electrons transferred from the metal-oxide interface. The efficiency to distribute the excess electrons becomes comparable in the two aggregates, as the terminal atoms holding large fractions of the charge are sufficiently separated in both cases (Fig. 5). However, the flat structure enables the formation of three additional Au-Au bonds, which makes this isomer finally more stable than the chain and indicates the crossover to the 2D growth regime.

III. DISCUSSION

The calculated preference for the formation of ultrasmall Au clusters with linear shapes is unambiguously confirmed by the experimental observations. After deposition of 0.02 ML Au onto MgO/Ag(001) thin films, small Au chains are the predominant adstructures besides individual adatoms. The analysis of STM images taken in several experimental runs reveals that trimer and tetramer chains are the most frequently found linear species on the surface. This observation is in agreement with the high formation energies of linear Au_3 ($E_b=0.94$) and Au_4 clusters (0.8 eV) (Fig. 6). In contrast, the formation energy exhibits a pronounced minimum for Au_5 chains, whose synthesis out of a Au_4 cluster is equally probable as its reorganization into a compact Au_5 cluster. In accordance, Au_5 chains are hardly found on the surface. The fact that even longer chains are experimentally observed only emphasizes the metastable character of the pentamer chain and its high tendency to transform into linear or 2D Au_6 clusters via atom attachment.

The longest chains identified in the STM images are Au_6 (two exemplars) and Au_7 species (one exemplar), which already coexist with various 2D clusters of approximately the same size. The experimentally determined transition between 1D and 2D growths therefore occurs for six to seven atoms in the Au aggregates. This number is in good agreement with the DFT results (five to six atoms) and the small discrepancy might be related to kinetic effects of the chain formation that are not accounted for in theory. Interestingly, the same critical size for the crossover in the growth regime has earlier been determined for Au aggregates on alumina/NiAl(110),[27] suggesting a certain universality of the underlying effect: The change from 1D to 2D growth mode occurs when the energy surplus from delocalizing the excess charges is outweighed by the formation of additional Au-Au bonds in compact 2D and 3D aggregates.

Finally, the absence of peaks in the dI/dV spectra of Au chains on thin MgO films shall be commented, in particular because a set of eigenstates was detected for similar adchains on alumina/NiAl.[27] The main difference between both systems is the increased sensitivity of MgO-supported Au chains against electron or hole injection from the tip, which limits the available bias range for spectroscopy to ± 1 V (compared to ± 3 V for alumina/NiAl). The large stability of alumina supported aggregates at high bias combines two effects.[27] Due to an unusual interaction mechanism that involves the cleavage of an Al-O bond, Au atoms are able to bind stronger to alumina than to magnesia films. Furthermore, the adchains form a surface complex with the topmost Al atoms of the alumina film, which enables a better delocalization of the charges injected from the tip and reduces the temporal Coulomb repulsion within the adchain and to the oxide support. The only detectable features in dI/dV maps of linear Au clusters on 2 ML MgO on Ag(001) are the pronounced end states located at both sides of the chains (Fig. 3). This increase in occupied state density might be related to the localization of excess electrons at the terminal chain atoms that has been deduced from the DFT calculations (Fig. 5). The presence of zero-dimensional end states might therefore provide another hint for the negative charging of the Au chains on the MgO film.

IV. CONCLUSION

Employing STM and DFT, we have demonstrated that ultrasmall gold clusters formed on thin MgO films on Ag(001) adopt a linear geometry. This particular cluster shape has no counterpart in the gas phase or on bulk

MgO(001) surfaces but is the consequence of the interaction between the adclusters and the metal support below the oxide film. The driving force for the chain formation is a charge transfer through the thin film into the Au clusters that satisfies the strong electronegative character of gold. The excess charges, amounting to two extra electrons for Au_4 to Au_6 chains, enable a strong polarization interaction with the oxide support but simultaneously enforce the linear arrangement of the atoms in order to minimize the internal Coulomb repulsion. As the growth of Au chains is also observed on alumina thin films, it might reflect a general trend in gold nucleation on those oxide films that support formation of anionic Au species.

It would be highly desirable to verify the charged nature of the Au clusters via an independent experimental technique. Several observables are sensitive to the charge state of adsorbates, for instance the energy position of core levels in photoelectron spectroscopy, the vibrational signature of probe molecules such as CO, and the work function change induced by charged adspecies. However, the detection of the charge state of Au clusters via spatially averaging methods might be extremely difficult due to their small abundance on the MgO film and is beyond the scope of this paper.

*nilius@fhi-berlin.mpg.de

†gianfranco.pacchioni@unimib.it

[1] M. Chen and D. W. Goodman, Acc. Chem. Res. **39**, 739 (2006).

[2] M. Haruta, T. Kobayashi, H. Sano, and N. Yamada, Chem. Lett. **2**, 405 (1987).

[3] M. Haruta, CATTECH **6**, 102 (2002).

[4] S. Arrii, F. Morfin, A. J. Renouprez, and J. L. Rousset, J. Am. Chem. Soc. **126**, 1199 (2004).

[5] N. Lopez and J. Norskov, J. Am. Chem. Soc. **124**, 11262 (2002).

[6] J. Guzman and B. C. Gates, Nano Lett. **1**, 689 (2001).

[7] Z.-P. Liu, S. J. Jenkins, and D. A. King, Phys. Rev. Lett. **94**, 196102 (2005).

[8] J. G. Wang and B. Hammer, Phys. Rev. Lett. **97**, 136107 (2006).

[9] L. D. Socaciu, J. Hagen, T. M. Bernhardt, L. Wöste, U. Heiz, H. Häkkinen, and U. Landman, J. Am. Chem. Soc. **125**, 10437 (2003).

[10] B. Yoon, H. Häkkinen, U. Landman, A. S. Wörz, J. Antonietti, S. Abbet, J. Judai, and U. Heiz, Science **307**, 403 (2005).

[11] L. M. Molina and B. Hammer, J. Catal. **233**, 399 (2005).

[12] D. Matthey, J. W. Wang, S. Wendt, J. Matthiesen, R. Schaub, E. Laegsgaard, B. Hammer, and F. Besenbacher, Science **315**, 1692 (2007).

[13] M. Sterrer, M. Yulikov, E. Fishbach, M. Heyde, H.-P. Rust, G. Pacchioni, T. Risse, and H.-J. Freund, Angew. Chem., Int. Ed. **45**, 2630 (2006).

[14] A. S. Wörz, U. Heiz, F. Cinquini, and G. Pacchioni, J. Phys. Chem. B **109**, 18418 (2005).

[15] G. Pacchioni, L. Giordano, and M. Baistrocchi, Phys. Rev. Lett. **94**, 226104 (2005).

[16] L. Giordano, G. Pacchioni, J. Goniakowski, N. Nilius, E. D. L. Rienks, and H.-J. Freund, Phys. Rev. Lett. **101**, 026102 (2008).

[17] L. Giordano, F. Cinquini, and G. Pacchioni, Phys. Rev. B **73**, 045414 (2006).

[18] H.-C. Ploigt, C. Brun, M. Pivetta, F. Patthey, and W.-D. Schneider, Phys. Rev. B **76**, 195404 (2007).

[19] H. M. Benia, N. Nilius, and H.-J. Freund, Surf. Sci. **601**, L55 (2007).

[20] N. Cabrera and N. F. Mott, Rep. Prog. Phys. **12**, 163 (1949).

[21] M. Sterrer, T. Risse, U. Martinez Pozzoni, L. Giordano, M. Heyde, H.-P. Rust, G. Pacchioni, and H.-J. Freund, Phys. Rev. Lett. **98**, 096107 (2007).

[22] M. Sterrer, T. Risse, M. Heyde, H.-P. Rust, and H.-J. Freund, Phys. Rev. Lett. **98**, 206103 (2007).

[23] D. Ricci, A. Bongiorno, G. Pacchioni, and U. Landman, Phys. Rev. Lett. **97**, 036106 (2006).

[24] P. Frondelius, H. Häkkinen, and K. Honkala, Phys. Rev. B **76**, 073406 (2007).

[25] P. Frondelius, H. Häkkinen, and K. Honkala, New J. Phys. **9**, 339 (2007).

[26] M. Kulawik, N. Nilius, and H.-J. Freund, Phys. Rev. Lett. **96**, 036103 (2006).

[27] N. Nilius, M. V. Ganduglia-Pirovano, V. Brazdova, M. Kulawik, J. Sauer, and H. J. Freund, Phys. Rev. Lett. **100**, 096802 (2008).

[28] C. Zhang, B. Yoon, and U. Landman, J. Am. Chem. Soc. **129**, 2228 (2007).

[29] H.-J. Freund, Surf. Sci. **601**, 1438 (2007).

[30] M. Heyde, M. Kulawik, H.-P. Rust, and H.-J. Freund, Rev. Sci. Instrum. **75**, 2446 (2004).

[31] V. Simic-Milosevic, M. Heyde, N. Nilius, T. König, H.-P. Rust, M. Sterrer, T. Risse, H.-J. Freund, L. Giordano, and G. Pacchioni, J. Am. Chem. Soc. **130**, 7814 (2008).

[32] J. P. Perdew, J. A. Chevary, S. H. Vosko, K. A. Jackson, M. R. Pederson, D. J. Singh, and C. Fiolhais, Phys. Rev. B **46**, 6671 (1992).

[33] G. Kresse and J. Hafner, Phys. Rev. B **47**, 558 (1993).

[34] G. Kresse and J. Furthmüller, Phys. Rev. B **54**, 11169 (1996).

[35] P. E. Blöchl, Phys. Rev. B **50**, 17953 (1994).

[36] H. J. Monkhorst and J. D. Pack, Phys. Rev. B **13**, 5188 (1976).

[37] A. Del Vitto, G. Pacchioni, F. Delbecq, and P. Sautet, J. Phys. Chem. B **109**, 8040 (2005).

[38] K. J. Taylor, C. L. Pettiette-Hall, O. Cheshnovsky, and R. E. Smalley, J. Chem. Phys. **96**, 3319 (1992).

[39] G. Barcaro and A. Fortunelli, J. Chem. Theory Comput. **1**, 972 (2005).

[40] L. M. Molina and J. A. Alonso, J. Phys. Chem. C **111**, 6668 (2007).